The C-terminal segment of Leishmania major HslU: Toward potential inhibitors of LmHslVU activity

Priyanka Singh, Krishnananda Samanta, Ndeye Mathy Kebe, Grégory Michel, Baptiste Legrand, Vera Sitnikova, Andrey Kajava, Michel Pagès, Patrick Bastien, Christelle Pomares, et al.

The C-Terminal Segment of *Leishmania major* HslU: toward Potential Inhibitors of LmHslVU Activity

Priyanka Singh,[a,#] Krishnananda Samanta,[a,#] Ndeye Mathy Kebe,[b] Grégory Michel,[c] Baptiste Legrand,[a] Vera E. Sitnikova,[d] Andrey V. Kajava,[b] Michel Pagès, [e,†] Patrick Bastien,[e] Christelle Pomares,[c] Olivier Coux[b,*] and Jean-François Hernandez[a,*]

[a]IBMM, CNRS, Univ Montpellier, ENSCM, Montpellier, France. [b]Centre de Recherche en Biologie Cellulaire de Montpellier (CRBM), UMR5237, CNRS, Univ Montpellier, 1919, route de Mende, 34000 Montpellier, France. [c]Centre Méditerranéen de Médecine Moléculaire (C3M), U1065, Université Côte d'Azur, Inserm, Archimed Building, 151 route Saint Antoine de Ginestière, 06000 Nice, France. [d]International Research Institute of Bioengineering, ITMO University, Kronverksky Pr. 49, 197101 Saint Petersburg, Russia. [e]MIVEGEC, Univ Montpellier, CNRS, IRD, CHU, 191 avenue du Doyen Giraud, 34000 Montpellier, France.

[#]PS and KS have performed equally.
[†]*In memoriam*

**E-mail addresses:* jean-francois.hernandez@umontpellier.fr (J.-F. Hernandez), olivier.coux@crbm.cnrs.fr (O. Coux)

Keywords: HlsV protease, Leishmania, medicinal chemistry, peptides, structure-activity relationships.

Abstract.

It is urgent to develop less toxic and more efficient treatments for leishmaniases and trypanosomiases. We explore the possibility to target the parasite mitochondrial HslVU protease, which is essential for growth and has no analogue in the human host. For this, we develop compounds potentially inhibiting the complex assembly by mimicking the C-terminal (C-ter) segment of the ATPase HslU. We previously showed that a dodecapeptide derived from *Leishmania major* HslU C-ter segment (LmC12-U2, Cpd **1**) was able to bind to and activate the digestion of a fluorogenic substrate by LmHslV. Here, we present the study of its structure-activity relationships. By replacing each essential residue with related non-proteinogenic residues, we obtained more potent analogues. In particular, a cyclohexylglycine residue at position 11 (cpd **24**) allowed a more than three-fold gain in potency while reducing the size of compound **24** from twelve to six residues (cpd **50**) without significant loss of potency, opening the way toward short HslU C-ter peptidomimetics as potential inhibitors of HslV proteolytic function. Finally, conjugates constituted of LmC6-U2 analogues and a mitochondrial penetrating peptide were found to penetrate into the promastigote form of *L. infantum* and to inhibit the parasite growth without showing toxicity toward human THP-1 cells at the same concentration (i.e. 30 μM).

1. Introduction.

Leishmaniases and trypanosomiases are worldwide spreading diseases caused by the parasitic protozoa *Leishmania* and *Trypanosoma*, respectively. These Trypanosomatid parasites mainly affect sub-tropical and tropical zones and significantly contribute to human misery in these regions. About 350 million people are at risk for leishmaniases. With 1.5-2 million new cases per year and annual mortality of about 60,000 mainly due to visceral leishmaniasis, the rise in the number of cases is alarming [1]. A recent concern is the sharp increase in the overlapping of HIV infection and visceral leishmaniasis. Particularly worrying in Africa, this co-infection also caused an increased incidence of this disease in southern Europe (Spain, France, Italy, Portugal) [2]. About 70 million persons are at risk for African (sleeping sickness, *T. brucei*) and 25 million for American (Chagas' disease, *T. cruzi*) trypanosomiases [3,4]. The African disease has largely regressed during the last decade due to control programs but the risk of major epidemic remains. *T. cruzi* infects 6-7 million people and kills 10,000 persons every year [4-6].

There is as yet no effective treatment against any form of these human diseases. Current drugs generally suffer of several drawbacks, including toxicity, administration complexity, resistance, inability to treat all forms of the diseases, and cost [7]. New safe and effective drugs are thus urgently needed. Whereas the interest of pharmaceutical companies to develop new drugs has been traditionally scarce as these diseases are mainly prevalent in the poorest areas of the world, important actions have been implemented since the beginning of the century to fight these neglected diseases. For instance, leishmaniases and trypanosomiases are the main targets of the not-for-profit organization "Drugs for Neglected Diseases *initiative*" (DND*i*, dndi.org), which enables research and development networks between academic and private partners.

Ideally these new drugs should be effective against both types of parasites and in both stages of the parasite life cycle (i.e. promastigote and amastigote for *Leishmania*, trypomastigote and amastigote for *Trypanosoma*).

The biology of trypanosomatids has been intensively studied and their genomes fully sequenced [8-10]. These organisms use many unique and atypical molecular and biochemical pathways, which may be exploited as potential drug targets [11].

The ATP-dependent HslVU protease complex is one of these interesting targets. First characterized in eubacteria [12-14], absent in higher eukaryotes, HslVU was found in ancestral eukaryotes like *Plasmodium* [15,16] and Trypanosomatids [17] with a mitochondrial

localization [18-20]. Studies by us [20] and others [18] have shown that HslVU plays an essential role for cell growth and survival in *Leishmania* and *Trypanosoma*. Thus, inhibiting HslVU may be a promising approach to cure these diseases. Because HslV and the human proteasome have the same catalytic mechanism and binding sites with wide specificity, targeting their active sites appears a risky approach to identify selective inhibitors. An alternative consists in the inhibition of HslV/HslU association, which is essential for activity of the protease [12].

HslVU is the assembly of two stacked hexameric rings of the threonine protease HslV, which are capped on both side by an hexameric ring of the ATPase HslU. HslU recognizes and unfolds protein substrates and translocates them into the internal proteolytic chamber of the HslV dodecamer. X-ray structures of bacterial HslVU complexes [21,22] and functional studies [23-25] have evidenced the role of the C-terminal segment (C-ter) of HslU in protease activation. By inserting into the HslV complex, HslU C-ters induce a conformational rearrangement of HslV that propagates to the active sites [26]. This allosteric activation mechanism differs from that of the eukaryotic proteasome, for which binding of activators opens a gated channel that controls access of substrates to the proteolytic chamber. These functional studies also showed the importance of HslU C-ter in the stability of HslVU and hexameric HslU complexes. A synthetic octapeptide derived from *Haemophilus* HslU C-terminus was shown to bind HslV and to potently activate the digestion of a small fluorogenic substrate but not proteins, which necessitate prior unfolding by HslU [23]. A similar result was obtained with *Leishmania*, for which the activation of HslV is accompanied by large conformational rearrangements of the complex [27]. This interaction is specific as substitution of the strictly conserved C-terminal leucine residue by an alanine abolishes HslV activation. HslU C-ter from eubacteria and protozoan parasites is highly conserved, strongly supporting that an identical mechanism operates. It is noteworthy that HslU and HslV have only a moderate affinity (K_d = 1 μM) for each other in the absence of substrate [28] probably because the HslU C-ter is buried in the HslU complex in these conditions [29]. This low affinity is an advantage for developing competing molecules based on the C-terminal segment of HslU. In support, a synthetic dodecapeptide derived from *P. falciparum* HslU C-ter was shown to compete with PfHslU for binding to PfHslV [30].

Intriguingly, in Trypanosomatids only, two HslU proteins, termed U1 and U2 co-exist. U1 and U2 are highly homologous in sequence except in the so-called I-domain thought to be involved in substrate recognition. The respective roles of U1 and U2 are not known. We

previously found that inhibition of the expression of HslU1 and HslU2 from *Trypanosoma brucei* yielded different phenotypes and that only HslU1 was indispensable to parasite survival [20]. In this context, Sung et al. reported that only a C-terminal octapeptide derived from HslU2 of *T. brucei* (TbHslU2) and not from TbHslU1 was able to activate the peptidolytic activity of TbHslV [31].

We recently described the production, purification and biochemical characterization of HslV from *Leishmania major* (LmHslV) [27]. In contrast to Sung's result, we showed that octapeptides as well as dodecapeptides derived from both LmHslU1 and LmHslU2 were able to activate LmHslV, although the activation was indeed more efficient with LmHslU2 peptides. In addition, we found that the corresponding dodecapeptides from EcHslU, TbHslU2 and PfHslU were also able to activate LmHslV, sometimes with higher efficiency than the LmHslU2 peptide itself. This result suggested that a same HslU Cter mimetic could target HslV of all microorganisms. Finally, based on a C-terminal U2-derived dodecapeptide chosen as a reference (i.e. LmC12-U2, H-arg-O2Oc-Leu-Gln-Lys-Asn-Val-Asn-Leu-Ala-Lys-Tyr-Leu-Leu-OH, Cpd **1**, Figure 1), we found that five out of its six C-terminal residues were essential for HslV binding and activation and that side-chain to side-chain cyclisation allowed reducing the peptide size from 12 to 9 residues without loss of potency.

H-*arg*-*O2Oc*-Leu-Gln-Lys-Asn-Val-Asn-**Leu**^{7}-Ala-**Lys**^{9}-**Tyr**^{10}-**Leu**^{11}-**Leu**^{12}-OH

Figure 1. Sequence of the reference activating peptide, LmC12-U2. Essential residues are in bold. The *N*-terminal segment arg-O2Oc provides better aqueous solubility.

Here, based on these results, we present an extended and extensive study of the structure-activity relationships of LmC12-U2 with the objective to obtain more potent analogues and to significantly reduce the size of HslU Cter mimetics. Finally, having identified potent LmC6-U2 analogues, conjugates with mitochondrial penetrating peptides (MPP) as well as fluorescently-labelled analogues were prepared and tested on *Leishmania infantum* cultures.

2. Results and Discussion

All peptides were assembled on a 2-chloro-trityl resin with Fmoc as the *N*α-protecting group and HBTU or HATU as coupling agents as already described [27].

Their ability to activate LmHslV was assessed using the fluorogenic substrate Z-EVNL-AMC (JMV4482) [27], which we found much more efficient than the Z-GGL-AMC substrate classically used to study HslVU [12]. As previously published, LmHslV displayed no activity

in the absence of peptides [27]. It gained activity in the presence of C-ter HslU peptides as already reported for bacterial HslV and TbHslV [23,31]. Peptides were compared based on the initial velocity of Z-EVNL-AMC digestion by LmHslV and results are reported as percentage of the initial velocity measured in the presence of the reference LmC12-U2 (Cpd **1**) in most experiments (Tables 1-3).

2.1. Structure-activity relationships of LmC12-U2

Five out of the six C-terminal residues of LmC12-U2 (Cpd **1**, Figure 1) were found to be essential for binding to and activation of LmHslV [27]. We considered that the essential nature of these residues was related to their tight interaction with well-defined pockets at the interface of two HslV subunits. With the objective to better define the structural requirements of LmHslU2 binding to LmHslV and to possibly obtain more efficient analogues, we individually substituted each essential position by structurally close and/or bulkier and mostly non-natural amino acids (Figure 2, Tables 1-3).

In addition, as even structurally close residues display slightly different physico-chemical properties, hydrophobicity and bulkiness, these changes may lead to a gain in affinity. Leucine residues (positions 7, 11 and 12) were mainly replaced by bulkier and more hydrophobic aliphatic amino acids such as cyclohexylalanine (Cha) or cyclohexylglycine (Chg). Lysine at position 9 was replaced by other basic residues or isosteric neutral ones. Tyrosine at position 10 was replaced by numerous aromatic residues more or less bulky and hydrophobic (Figure 2). We assumed that a higher activation level would reflect a higher affinity, although we cannot rule out that it could result from a more efficient substrate binding or catalytic activity.

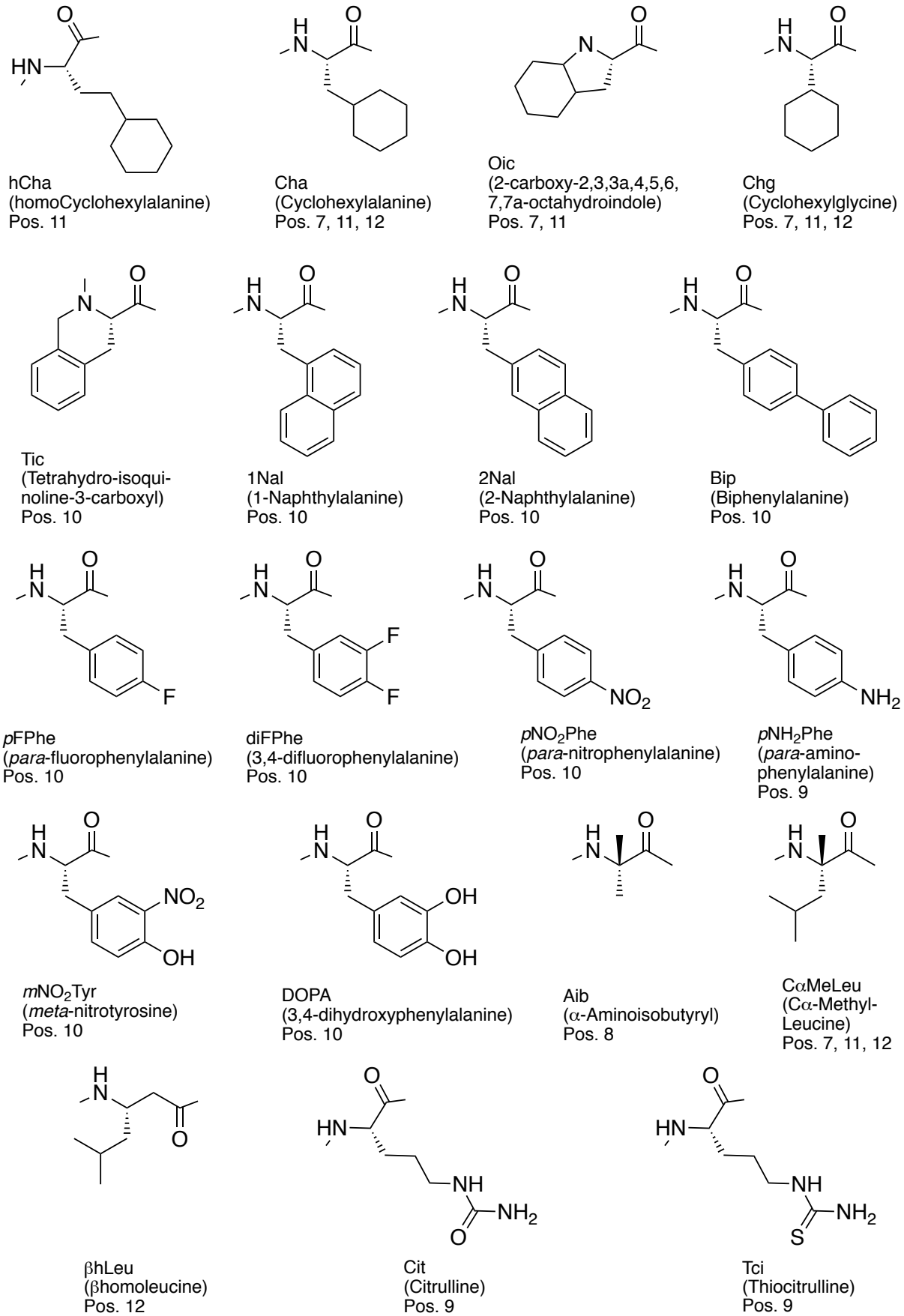

Figure 2. Structure of the non-proteinogenic amino acid residues used in this study. The positions (7, 8, 9, 10, 11 or 12) where they have been individually introduced are indicated.

Table 1. LmHslU2 C-ter peptide mono-and multisubstituted analogues 1-35 and their LmHslV activation potency at 500 μM.

Cpd	Structure	Name	Relative potency (%)[a]
1	H-*arg-O2Oc*-Leu[1]-Gln-Lys-Asn-Val-Asn-Leu[7]-Ala-Lys[9]-Tyr[10]-Leu[11]-Leu[12]-OH	LmC12-U2	100
Monosubstituted analogues			
Position 7			
2	H-*arg-O2Oc*-Leu-Gln-Lys-Asn-Val-Asn-**Cha**-Ala-Lys-Tyr-Leu-Leu-OH	[Cha[7]]-LmC12-U2	91 ± 1
3	H-*arg-O2*Oc-Leu-Gln-Lys-Asn-Val-Asn-**Chg**-Ala-Lys-Tyr-Leu-Leu-OH	[Chg[7]]-LmC12-U2	92 ± 14
4	H-*arg-O2Oc*-Leu-Gln-Lys-Asn-Val-Asn-**Oic**-Ala-Lys-Tyr-Leu-Leu-OH	[Oic[7]]-LmC12-U2	17 ± 1
Position 9			
5	H-*arg-O2Oc*-Leu-Gln-Lys-Asn-Val-Asn-Leu-Ala-**Orn**-Tyr-Leu-Leu-OH	[Orn[9]]-LmC12-U2	15 ± 1
6	H-*arg-O2Oc*-Leu-Gln-Lys-Asn-Val-Asn-Leu-Ala-***p*NH$_2$Phe**-Tyr-Leu-Leu-OH	[*p*NH$_2$Phe[9]]-LmC12-U2	99 ± 9
7	H-*arg-O2Oc*-Leu-Gln-Lys-Asn-Val-Asn-Leu-Ala-**Arg**-Tyr-Leu-Leu-OH	[Arg[9]]-LmC12-U2	103 ±6
8	H-*arg-O2Oc*-Leu-Gln-Lys-Asn-Val-Asn-Leu-Ala-**Cit**-Tyr-Leu-Leu-OH	[Cit[9]]-LmC12-U2	53 ± 8
9	H-*arg-O2Oc*-Leu-Gln-Lys-Asn-Val-Asn-Leu-Ala-**Tci**-Tyr-Leu-Leu-OH	[Tci[9]]-LmC12-U2	83 ± 8
Position 10			
10	H-*arg-O2Oc*-Leu-Gln-Lys-Asn-Val-Asn-Leu-Ala-Lys-**Phe**-Leu-Leu-OH	[Phe[10]]-LmC12-U2	13 ± 2
11	H-*arg-O2Oc*-Leu-Gln-Lys-Asn-Val-Asn-Leu-Ala-Lys-**Tic**-Leu-Leu-OH	[Tic[10]]-LmC12-U2	NA[b]
12	H-*arg-O2Oc*-Leu-Gln-Lys-Asn-Val-Asn-Leu-Ala-Lys-***p*FPhe**-Leu-Leu-OH	[*p*FPhe[10]]-LmC12-U2	17 ± 2
13	H-*arg-O2Oc*-Leu-Gln-Lys-Asn-Val-Asn-Leu-Ala-	[diFPhe[10]]-	28 ± 3

	Lys-**diFPhe**-Leu-Leu-OH	LmC12-U2	
14	H-*arg*-*O2Oc*-Leu-Gln-Lys-Asn-Val-Asn-Leu-Ala-Lys-***p*NO₂Phe**-Leu-Leu-OH	[*p*NO_2Phe[10]]-LmC12-U2	26 ± 4
15	H-*arg*-*O2Oc*-Leu-Gln-Lys-Asn-Val-Asn-Leu-Ala-Lys-***m*NO₂Tyr**-Leu-Leu-OH	[*p*NO_2Tyr[10]]-LmC12-U2	58 ± 10
16	H-*arg*-*O2Oc*-Leu-Gln-Lys-Asn-Val-Asn-Leu-Ala-Lys-**DOPA**-Leu-Leu-OH	[DOPA[10]]-LmC12-U2	139 ± 13
17	H-*arg*-*O2Oc*-Leu-Gln-Lys-Asn-Val-Asn-Leu-Ala-Lys-**1Nal**-Leu-Leu-OH	[1Nal[10]]-LmC12-U2	166 ± 5
18	H-*arg*-*O2Oc*-Leu-Gln-Lys-Asn-Val-Asn-Leu-Ala-Lys-**2Nal**-Leu-Leu-OH	[2Nal[10]]-LmC12-U2	115 ± 24
19	H-*arg*-*O2Oc*-Leu-Gln-Lys-Asn-Val-Asn-Leu-Ala-Lys-**Trp**-Leu-Leu-OH	[Trp[10]]-LmC12-U2	136 ± 11
20	H-*arg*-*O2Oc*-Leu-Gln-Lys-Asn-Val-Asn-Leu-Ala-Lys-**Bip**-Leu-Leu-OH	[Bip[10]]-LmC12-U2	16 ± 4
Position 11			
21	H-*arg*-*O2Oc*-Leu-Gln-Lys-Asn-Val-Asn-Leu-Ala-Lys-Tyr-**Cha**-Leu-OH	[Cha[11]]-LmC12-U2	278 ± 24
22	H-*arg*-*O2Oc*-Leu-Gln-Lys-Asn-Val-Asn-Leu-Ala-Lys-Tyr-**Phe**-Leu-OH	[Phe[11]]-LmC12-U2	46 ± 7
23	H-*arg*-*O2Oc*-Leu-Gln-Lys-Asn-Val-Asn-Leu-Ala-Lys-Tyr-**hCha**-Leu-OH	[hCha[11]]-LmC12-U2	160 ± 23
24	H-*arg*-*O2Oc*-Leu-Gln-Lys-Asn-Val-Asn-Leu-Ala-Lys-Tyr-**Chg**-Leu-OH	[Chg[11]]-LmC12-U2	354 ± 17
25	H-*arg*-*O2Oc*-Leu-Gln-Lys-Asn-Val-Asn-Leu-Ala-Lys-Tyr-**Oic**-Leu-OH	[Oic[11]]-LmC12-U2	NA
26	H-*arg*-*O2Oc*-Leu-Gln-Lys-Asn-Val-Asn-Leu-Ala-Lys-**Phe**-**Chg**-Leu-OH	[Phe[10], Chg[11]]-LmC12-U2	350 ± 28
27	H-*arg*-*O2Oc*-Leu-Gln-Lys-Asn-Val-Asn-Leu-Ala-Lys-Tyr-**Chg**-**Ala**-OH	[Chg[11], Ala[12]]-LmC12-U2	36 ± 5
Position 12			
28	H-*arg*-*O2Oc*-Leu-Gln-Lys-Asn-Val-Asn-Leu-Ala-Lys-Tyr-Leu-**βhLeu-OH**	[βhLeu[12]]-LmC12-U2	NA
29	H-*arg*-*O2Oc*-Leu-Gln-Lys-Asn-Val-Asn-Leu-Ala-Lys-Tyr-Leu-**Cha**-OH	[Cha[12]]-LmC12-U2	26 ± 3
30	H-*arg*-*O2Oc*-Leu-Gln-Lys-Asn-Val-Asn-Leu-Ala-	[Chg[12]]-	105 ± 12

	Lys-Tyr-Leu-**Chg**-OH	LmC12-U2	
Multisubstituted analogues			
31	H-*arg-O2OC*-Leu-Gln-Lys-Asn-Val-Asn-Leu-Ala-**Arg**-Tyr-**Cha**-Leu-OH	[Arg^{9}, Cha^{11}]-LmC12-U2	203 ± 20
32	H-*arg-O2OC*-Leu-Gln-Lys-Asn-Val-Asn-Leu-Ala-**Arg**-**1Nal**-Leu-Leu-OH	[Arg^{9}, 1Nal^{10}]-LmC12-U2	146 ± 21
33	H-*arg-O2OC*-Leu-Gln-Lys-Asn-Val-Asn-Leu-Ala-Lys-**1Nal**-**Cha**-Leu-OH	[1Nal^{10}, Cha^{11}]-LmC12-U2	192 ± 10
34	H-*arg-O2OC*-Leu-Gln-Lys-Asn-Val-Asn-**Cha**-Ala-**Arg**-Tyr-**Cha**-Leu-OH	[Cha^{7}, Arg^{9}, Cha^{11}]-LmC12-U2	303 ± 24
35	H-*arg-O2OC*-Leu-Gln-Lys-Asn-Val-Asn-**Cha**-Ala-Lys-**1Nal**-**Cha**-Leu-OH	[Cha^{7}, 1Nal^{10}, Cha^{11}]-LmC12-U2	242 ± 18

[a]Percentage of initial velocity relative to compound **1** (100%). LmHslV (2 µg, 75.2 nM) was incubated at 37 °C with 100 µM JMV4482 (Z-EVNL-AMC) in the presence of 500 µM peptides. The fluorescence of the free AMC group, proportional to the activity of the sample, was measured at 2 min. intervals. [b]NA: no activity (<10%).
Bip = Biphenylalanine (*para*-Phenyl-Phenylalanine); Cha = CyclohexylAlanine; Chg = CyclohexylGlycine; Cit = Citrulline; diFPhe = 3,4-DifluoroPhenylalanine; DOPA = 3,4-DihydroxyPhenylalanine; *p*FPhe = *para*-FluoroPhenylalanine; hCha = homoCyclohexylAlanine; βhLeu = β-homoLeucine; 1Nal, 2Nal = 1-, 2-Naphthylalanine; *p*NH_2Phe = *para*-AminoPhenylalanine; *p*NO_2Phe = *para*-NitroPhenylalanine; *m*NO_2Tyr = *meta*-NitroTyrosine; O2Oc = [2-(2-aminoethoxy)ethoxy]acetyl; Oic = Octahydroindole-2-carboxyl; Orn = Ornithine; Tci = Thiocitrulline; Tic = Tetrahydroisoquinoline-3-carboxyl.

2.1.1. Monosubstituted analogues.

2.1.1.1 Substitutions at positions 7 or 9. Table 1 shows the activity of analogues mono-substituted at positions 7 or 9 relative to the reference **1**. The substitution of Leu^{7} by its closest analogue Cha (**2**) or the shorter Chg (**3**) had no effect on the activation level. In contrast, Oic (**4**), which is a proline analogue of Cha, led to a five-fold decrease in potency. This effect could be due to side-chain constraining and/or to the absence of a potential hydrogen bond between the peptide and HslV. In the case of Lys^{9}, changes showed that this residue binds to a large pocket in HslV and that a positive charge could be spared. Indeed, a minimal size is required as replacing Lys by its one-methylene shorter analogue Orn (**5**) decreased the activating potency by more than six-fold, while replacing it with the bulkier *p*-aminophenylalanine (**6**) yielded similar potency. As expected, the other natural basic residue Arg yielded a similarly efficient analogue (**7**). In HiHslVU (1G3I.pdb [21]), the residue equivalent to Lys^{9} is HiHslU Arg^{441}, whose side-chain faces an acidic environment formed by HiHslV Glu^{61} and Glu^{58} residues, which are conserved in LmHslV, suggesting important

ionic interaction. In contrast, replacing Lys^{9} by the isosteric but uncharged arginine analogues citrulline (**8**) and thiocitrulline (**9**) only slightly decreased the activating potency (relative potencies of 53% and 83%, respectively), suggesting that the urea group and in particular the bulkier thiourea group could compensate the absence of charge by their ability to establish several hydrogen bonds.

2.1.1.2. Substitutions at positions 10, 11, or 12. More dramatic variations were observed when substituting the last three residues Tyr-Leu-Leu. Substitution of Tyr^{10} led to disparate results (Table 1). As already reported, the replacement of this residue by Phe (**10**) led to a eight-fold decrease in activity [27]. In addition, introducing the constrained pipecolic analogue of Phe, 1,2,3,4-tetrahydroisoquinoline-3-carboxyl (Tic) (**11**), completely abolished HslV activation. Introducing various substituents on Phe (*p*-fluoro- **12**, 3,4-difluoro- **13**, *p*-nitro- **14**) only slightly increased the potency compared to **10** (up to less than 30% relative potency), but all three analogues were three- to five-fold less potent than the reference peptide, suggesting an important interaction between the tyrosine phenol group and HslV that could not be compensated by fluorine or nitro group. In fact, structural data obtained for TbHslV [31] and HiHslVU [21] suggest that the phenol group establishes H-bond(s) with Ala^{79} main chain atoms and/or Lys^{80} in HslV. In agreement with this, introducing substituents on Tyr led to less important changes and could be favourable to potency in some cases. Whereas the [*m*-nitroTyr^{10}]-LmC12-U2 analogue **15** was about half as potent as the parent peptide **1**, the DOPA (or *m*-hydroxyTyr)-containing compound **16** was 1.4-fold more potent. Overall, these results support the importance of the tyrosine hydroxyl group in HslV activation.

However, we found that the absence of the hydroxyl group can be balanced by bulky bicyclic aromatic residues. Indeed, the three analogues **17** ([1-Nal^{10}]), **18** ([2-Nal^{10}]) and **19** ([Trp^{10}]) were as or significantly more efficient than the reference peptide. In particular, **17** was the most potent of this series with a 1.6-fold increase in activity. **20** ([Bip^{10}]-) was an exception, indicating that the second phenyl group at the para position of Phe might not be well accommodated by the corresponding HslV interaction pocket.

More striking results were obtained when exploring position 11 (Table 1). First, replacing the leucine residue by its closest analogue Cha (**21**) led to an approximately 2.7-fold increase in potency compared to LmC12-U2 **1**. Interestingly, the corresponding aromatic residue Phe in compound **22** was much less favourable (2-fold less potent than LmC12-U2), indicating that the larger volume and/or higher adaptability of the cyclohexyl ring allowed a better recognition by HslV. Then, increasing the side-chain by one methylene (i.e. a homoCha

residue) yielded the less potent **23**, which nevertheless still proved better than compound **1** (1.6-fold more efficient). In contrast, shortening it by the same unit (i.e. a Chg residue) was more favourable to activity, with **24** being about 3.5-fold more potent than LmC12-U2. Replacing Cha by octahydroindolecarboxyl (Oic, compound **25**) abolished the activity, indicating that the Cha-like side-chain of Oic was blocked in an orientation not compatible with binding and/or that an essential hydrogen bond was lost. Finally, it is noteworthy that replacing the Tyr^{10} residue by Phe in the [Chg^{11}] analogue (**26**) did not lead to a lower level of activation compared to **24**. It is also striking that, although substitution of the C-terminal Leu residue by Ala (**27**) led to a ten-fold decrease in potency compared to **24**, the activity was not abolished in contrast to what was previously observed for [Ala^{12}]-LmC12-U2 [27]. **27** showed about 35% activity as compared with compound **1**. Overall, these results showed that the presence of a cyclohexyl ring at position 11 is of high interest but the structural basis of this particular behaviour is unclear.

Finally, as expected [23], the C-terminal Leu residue was confirmed to be critical to activate LmHslV. Indeed, introducing the β-amino acid residue β-homoLeu (**28**) abolished the activity. However, whereas substitution by the closest analogue Cha (**29**) caused a four-fold decrease in potency, replacing Leu^{12} by the shorter Chg (**30**) was fully tolerated.

2.1.2. Combined substitutions at positions 7, 9, 10, 11. The first part of the study showed that it was possible to modulate the activation potency of the reference peptide **1** LmC12-U2 by replacing essential residues with closely related ones. Moreover, more potent analogues were obtained with substitutions at positions 10 and 11, which could help the design of peptidomimetics. To check if the combination of several of these favourable substitutions could yield a synergetic effect, we prepared a few di- (**31**-**33**) and tri-substituted (**34**, **35**) analogues of LmC12-U2 diversely combining the neutral (i.e. no individual effect) [Cha^{7}], [Arg^{9}], and two of the most favourable mono-substitutions [$1Nal^{10}$] and [Cha^{11}] (Table 1). Unfortunately, compared to the corresponding mono-substituted peptides, most analogues showed lower activation potency. In particular, compound **33**, which contained two favorable substitutions ($1Nal^{10}$ and Cha^{11}) showed intermediate activity compared to the corresponding mono-substituted **17** and **21**. Interestingly, compound **35**, which differed from **33** by the presence of the neutral Cha at position 7 was 1.2-fold more potent than **33**. In addition, the tri-substituted analogue **34** ([Cha^{7}, Arg^{9}, Cha^{11}]), which combined two neutral and one favourable substitution was found to be slightly more potent (303% vs 278%) than the [Cha^{11}]-LmC12-U2 analogue **21**.

Our observation that most of the combined substitutions do not have a synergic effect can be explained by the assumption that each individual substitution causes slight adjustment of the peptides within the binding pocket. The synergy will be observed only in the cases when the adjustment induced by two or more combined substitutions occurs in the same direction.

2.1.3. Constrained analogues. When interacting with HslV, the C-terminal hexapeptide segment of HslU in *Hemophilus influenzae* forms a short helical structure, the C-terminal leucine residue being distended from this helix [21]. Various local and global conformational constraints have been introduced in order to favour this conformation (Table 2).

Table 2. LmHslU2 C-ter peptide constrained analogues 36-47 and their LmHslV activation potency at 500 μM.

Cpd	Structure	Name	Relative potency (%)[a]
1	H-*arg-O2Oc*-Leu[1]-Gln-Lys-Asn-Val-Asn-Leu[7]-Ala-Lys[9]-Tyr[10]-Leu[11]-Leu[12]-OH	LmC12-U2	100
Cα-Methyl-substituted analogues of LmC12-U2			
36	H-*arg-O2Oc*-Leu-Gln-Lys-Asn-Val-Asn-**CαMeLeu**-Ala-Lys-Tyr-Leu-Leu-OH	[CαMeLeu[7]]-LmC12-U2	103 ± 5
37	H-*arg-O2Oc*-Leu-Gln-Lys-Asn-Val-Asn-Leu-**Aib**-Lys-Tyr-Leu-Leu-OH	[Aib[8]]-LmC12-U2	52 ± 2
38	H-*arg-O2Oc*-Leu-Gln-Lys-Asn-Val-Asn-Leu-Ala-Lys-Tyr-**Cα-MeLeu**-Leu-OH	[CαMeLeu[11]]-LmC12-U2	NA
39	H-*arg-O2Oc*-Leu-Gln-Lys-Asn-Val-Asn-Leu-Ala-Lys-Tyr-Leu-**CαMeLeu**-OH	[CαMeLeu[12]]-LmC12-U2	NA
Cyclic analogues of LmC9-U2			
40	H-*arg-O2Oc*-c[**Asp**-Val-Asn-Leu-**Lys**]-Lys-Tyr-Leu-Leu-OH	c[Asp[4], Lys[8]]-LmC9-U2	100
41	H-*arg-O2Oc*-c[**Glu**-Val-Asn-Leu-**Lys**]-Lys-Tyr-Leu-Leu-OH	c[Glu[4], Lys[8]]-LmC9-U2	11 ± 2
42	H-*arg-O2Oc*-c[**Lys**-Val-Asn-Leu- **Asp**]-Lys-Tyr-Leu-Leu-OH	c[Lys[4], Asp[8]]-LmC9-U2	23 ± 5
43	H-*arg-O2OC*-c[**Asp**-Val-Asn-Leu-**Lys**]-**Arg**-Tyr-Leu-Leu-OH	c[Asp[4], Lys[8], Arg[9]]-LmC9-U2	59 ± 2

44	H-*arg*-*O2OC*-c[**Asp**-Val-Asn-Leu-**Lys**]-Lys-**1Nal**-Leu-Leu-OH	c[Asp^4, Lys^8, 1Nal^{10}]-LmC9-U2	87 ± 2
45	H-*arg*-*O2OC*-c[**Asp**-Val-Asn-Leu-**Lys**]-Lys-Tyr-**Cha**-Leu-OH	c[Asp^4, Lys^8, Cha^{11}]-LmC9-U2	136 ± 15
46	H-*arg*-*O2Oc*-c[**Asp**-Val-Asn-Leu- **Lys**]-Lys-Tyr-**Chg**-Leu-OH	c[Asp^4, Lys^8, Chg^{11}]-LmC9-U2	323 ± 39
47	H-*arg*-*O2Oc*-c[**Lys**-Val-Asn-Leu- **Asp**]-Lys-Tyr-**Chg**-Leu-OH	c[Lys^4, Asp^8, Chg^{11}]-LmC9-U2	326 ± 36

[a]Percentage of initial velocity relative to compound **1** (100%). LmHslV (2 µg, 75.2 nM) was incubated at 37 °C with 100 µM JMV4482 (Z-EVNL-AMC) in the presence of 500 µM peptides. The fluorescence of the free AMC group, proportional to the activity of the sample, was measured at 2 min. intervals. [b]NA: no activity (<10%).
Aib = α-aminoisobutyryl; CαMeLeu = Cα-Methyl-Leucine; Cha = CyclohexylAlanine; Chg = CyclohexylGlycine; 1Nal = 1-Naphthylalanine; O2Oc = [2-(2-aminoethoxy)ethoxy]acetyl.

First, the three leucine residues at positions 7, 11 and 12 as well as Ala^8 have been individually replaced by their Cα-methyl analogue (CαMethyl-Leucine (CαMeLeu) and α-aminoisobutyric acid (Aib), respectively). These amino acids have been shown to induce local constraints favouring either β-turn or helix secondary structures [32-35]. In addition, they could also provide the peptides with a higher resistance to enzyme degradation [36,37]. Unfortunately, the analogues **38** (CαMeLeu^{11}) and **39** (CαMeLeu^{12}) were devoid of activity, while analogue **37** (Aib^8) was half as potent as the reference peptide and a CαMeLeu at position 7 (**36**) did not induce any change (Table 2). To check the influence of these substitutions on peptide conformation, we studied compounds **1**, **36** and **37** by circular dichroism (CD) in aqueous buffer without or with increasing concentrations of trifluoroethanol (TFE), a co-solvent with helix-promoting properties (Figure S1 and Table S4). As already observed in our previous study [27], all peptides display random conformation with very low helix content (< 5% in the absence of TFE). Addition of TFE only slightly increased it further, reaching a maximum of 12% helix content at 50% TFE. Overall, all three peptides behaved quite identically (Figure S1 and Table S4), indicating that the substitution by Cα-methyl aminoacids in compounds **36** and **37** had no effect on the conformation when compared to the parent peptide **1**. These results may explain why no improvement in activity was observed following this approach. In addition, the decreased activity observed for compounds **37**-**39** indicated that the CαMethyl group might hinder some important interaction with HslV and confirmed the essential role of the last two C-terminal leucine residues.

Second, we further explored global conformational constraint through side-chain to side-chain cyclisation between positions 4 (i) and 8 (i + 4). We previously reported that cyclization between Asp^4 and Lys^8 through a lactam bridge in LmC12-U2 was well tolerated and that it was possible to decrease the size to the corresponding cyclic C9-U2 (**40**, see Table 2) without loss of potency [27]. We first substituted Asp^4 to Glu^4 to slightly increase the cycle size (compound **41**), and, as observed when decreasing it [27], this change led to a ten-fold loss in potency. These results indicated that the 20-atom ring formed by the (Asp^i, Lys^{i+4}) bridge is optimal for activity. The fact that it is also optimal for helix stabilization [38] suggests that it stabilizes at least one helix turn in LmC9-U2. We also reversed Asp and Lys residues (compound **42**) and decreased activity was also observed. This result was not unexpected as it has been reported that the orientation and/or the position of a lactam bridge could be critical for helix stability [39].

The next step was to combine the cyclic constraint with the most favourable amino acid substitutions described above. Several analogues of the cyclic C9-U2 peptide were prepared, including [Arg^9] (**43**), [$1Nal^{10}$] (**44**), [Cha^{11}] (**45**) and [Chg^{11}] (**46**) substituted compounds (Table 1). The two first analogues were found to be slightly less potent than the non-substituted cyclic C9-U2 peptide. In contrast, the [Cha^{11}] analogue **45** was found slightly more potent, but the observed 1.3-fold increase in activity was less notable than in the case of the linear LmC12-U2 reference peptide. More interestingly, the presence of a Chg residue at position 11 (**46**) strongly increased potency, being about three-fold more active than the parent cyclic peptide. In addition, the analogue **47** with a reverse lactam bridge was found as potent as **46**, in contrast to what was observed for compound **42**. These results confirmed the exceptional interest of Chg at this position.

2.1.4. From dodeca- to hexapeptide series. After having explored the structure-activity relationships using LmC12-U2 (compound **1**) as a reference, we checked if the highly favorable substitutions, i.e. [Chg^{11}] and [Cha^{11}] in analogues **24** and **21**, respectively, could be the basis of potent shortened analogues. As we previously showed that the minimal segment able to activate LmHslV was LmC6-U2 (**48**) [27], we first prepared the corresponding [Cha^{11}]- and [Chg^{11}]-LmC6-U2 analogues (**49** and **50**, respectively). Table 3 shows that half-shortening was very well tolerated in the case of the [Chg^{11}] analogue **50** compared to **24**, whereas the [Cha^{11}] analogue **49** was about three-fold less potent than the corresponding dodecapeptide **21** but still around six-fold more potent than the non-substituted LmC6-U2 **48**.

Table 3. LmHslU2 C-ter hexapeptide analogues 48-58 and their LmHslV activation potency at 500 μM.

Cpd	Structure	Name	Relative potency (%)[a]
1	H-*arg*-*O2Oc*-Leu[1]-Gln-Lys-Asn-Val-Asn-Leu[7]-Ala-Lys[9]-Tyr[10]-Leu[11]-Leu[12]-OH	LmC12-U2	100
LmC6-U2 and substituted analogues			
48	H-*arg*-*O2Oc*-Leu-Ala-Lys-Tyr-Leu-Leu-OH	LmC6-U2	17 ± 4
49	H-*arg*-*O2Oc*-Leu-Ala-Lys-Tyr-**Cha**-Leu-OH	[Cha[11]]-LmC6-U2	92 ± 39
50	H-*arg*-*O2Oc*-Leu-Ala-Lys-Tyr-**Chg**-Leu-OH	[Chg[11]]-LmC6-U2	300 ± 17
51	H-*arg*-*O2Oc*-Lys-Tyr-**Chg**-Leu-OH	[Chg[11]]-LmC4-U2	NA
52	H-*arg*-*O2Oc*-γLeu-Lys-Tyr-**Chg**-Leu-OH	[γLeu[8], Chg[11]]-LmC5-U2	52 ± 13
53	H-*arg*-*O2Oc*-Leu-Ala-Lys-**1Nal**-**Chg**-Leu-OH	[1Nal[10], Chg[11]]-LmC6-U2	310 ± 56
54	H-*arg*-*O2Oc*-Leu-Ala-Lys-**2Nal**-**Chg**-Leu-OH	[2Nal[10], Chg[11]]-LmC6-U2	310 ±80
55	H-*arg*-*O2Oc*-Leu-Ala-Lys-**DOPA**-**Chg**-Leu-OH	[DOPA[10], Chg[11]]-LmC6-U2	228 ± 35
56	H-arg-O2Oc-Leu-Ala-Lys-***m*NO$_2$Tyr**-**Chg**-Leu-OH	[*m*NO$_2$Tyr[10], Chg[11]]-LmC6-U2	76 ± 11
57	H-*arg*-*O2Oc*-Leu-Ala-Lys-Tyr-**Chg**-**Chg**-OH	[Chg[11,12]]-LmC6-U2	317 ± 47
58	H-*arg*-*O2Oc*-Leu-Ala-Lys-Tyr-**Chg**-**Ala**-OH	[Chg[11], Ala[12]]-LmC6-U2	NA

[a]Percentage of initial velocity relative to compound **1** (100%). LmHslV (2 μg, 75.2 nM) was incubated at 37 °C with 100 μM JMV4482 (Z-EVNL-AMC) in the presence of 500 μM peptides. The fluorescence of the free AMC group, proportional to the activity of the sample, was measured at 2 min. intervals. [b]NA: no activity (<10%).
Cha = CyclohexylAlanine; Chg = CyclohexylGlycine; DOPA = 3,4-DihydroxyPhenylalanine; 1Nal, 2Nal = 1-, 2-Naphthylalanine; *m*NO$_2$Tyr = *meta*-NitroTyrosine; O2Oc = [2-(2-aminoethoxy)ethoxy]acetyl.

We also confirmed that the hexapeptidic length was required as the tetrapeptide [Chg[11]]-C4-U2 (**51**) was inactive. Nevertheless, it is interesting to note that the pseudo-pentapeptide **52**

where the dipeptide Leu^{7}-Ala^{8} was replaced by a γLeu residue displayed significant activity (about 50% that of LmC12-U2). Overall, Chg was much more efficient than Cha, and **50** was approximately three-fold and seventeen-fold more potent than LmC12-U2 and LmC6-U2, respectively.

Analogues of compound **50** were prepared where Tyr^{10} and/or Leu^{12} were replaced by close residues (1-Nal (**53**), 2-Nal (**54**), DOPA (**55**) and *m*-nitroTyr (**56**) at position 10; Chg residue (**57**) at position 12). Table 3 showed that no analogue was found significantly more potent than **50**, while substituting Leu^{12} with an Ala residue (**58**) abolished activity as expected.

Assuming that a better activation potency relates to stronger binding, we tried to understand the higher activity of Chg^{11}-containing analogues by molecular modelling. The compounds LmC8-U2 and [Chg^{11}]-LmC8-U2 were modelled into the HslU C-ter-binding site situated between two subunits of the HslV complex from *Leishmania*. The *Leishmania*-based models were generated using the known structure of the HslVU complex from *Haemophilus influenza* (i.e. HiHslVU, PDB code 1G3I [21]) and INSIGHT II program [40]. The modelling showed that both Chg^{11} and Leu^{11} fit similarly the binding pocket (see Figure S2 for the Chg^{11}-containing segment) and no clear difference in binding energy could be observed in this study. One hypothesis is that Chg imposes a higher rigidity to the peptide leading to a difference in the binding kinetics, which could impact the activation mode. This hypothesis is in line with the fact that Chg is a β-branched residue (not the case of Leu) and its lateral chain is further constrained by cyclisation and thus less mobile, which in turn could be an advantage to rapidly fit in the binding site, provided that is has the right orientation.

2.2. In vitro activity against the promastigote form of Leishmania infantum

We studied whether the most potent hexapeptide compound found here, **50** ([Chg^{11}]-LmC6-U2), could impair parasites' survival in culture.

It is generally admitted that such peptides are not able to cross cell membranes. In addition, to reach its target HslVU, the compound has to cross both the cell and mitochondrion membranes. Thus, we considered to conjugate the peptide to a cell penetrating peptide (CPP). This approach has already been reported to target the HslVU complex of *Plasmodium falciparum* (PfHslVU) [30]. In this study, the Authors attached the well-known 16-residues-long CPP penetratin to the PfHslU C-terminal dodecapeptide (i.e. PfC12-U), and the resulting conjugate was shown to inhibit parasite growth in a dose-dependent manner. However, this conjugate is long (28 residues) and therefore highly exposed to proteolytic degradation. In

addition, the C-terminal HslU segment was not optimized and penetratin is not considered to preferentially target the mitochondrion. We therefore conjugated the hexapeptidic segment of **50** to another CPP belonging to a family of mitochondrial penetrating peptides (MPPs), which have been shown to specifically localize and to deliver small peptidic cargoes to mitochondria in human cell [41-44].

Table 4. Fluorescently-labelled MPP's 59-68.

Cpd	Structure[a]	Ref.
59	TO-arg-Phe-Lys-Phe-NH_2	
60	TO-Phe-arg-Phe-Lys-NH_2	[41]
61	FITC-*Ahx*-Phe-arg-Phe-Lys-NH_2	
62	TO-Cha-arg-Cha-Lys-NH_2	[42]
63	FITC-*Ahx*-Cha-arg-Cha-Lys-NH_2	
64	TO-Cha-arg-Cha-Lys-Cha-arg-Cha-Lys-NH_2	[42]
65	FITC-*Ahx*-Cha-arg-Cha-Lys-Cha-arg-Cha-Lys-NH_2	
66	TO-Cha-arg-Cha-arg-NH_2	[46]
67	TO-Cha-arg-Cha-arg-Cha-arg-NH_2	[46]
68	FITC-*Ahx*-Cha-arg-Cha-arg-Cha-arg-NH_2	

[a]Axh = 6-aminohexanoyl; Cha = cyclohexylalanine; FITC = fluorescein-isothiocyanate; TO = thiazole orange.

First, we checked if MPPs could indeed enter in the parasite cell and mitochondrion. In contrast to higher eukaryotes, parasitic protozoa (e.g. *Leishmania*, *Trypanosoma*, *Plasmodium*) often exhibit a single large mitochondrion with a membrane composition similar to that of higher eukaryote mitochondria. We synthesized several fluorescently-labelled MPP's (Table 4). Two fluorophores were studied, *i.e.* thiazole orange (TO) [45] and fluorescein (FITC), which were conjugated at the N-terminus of MPPs. In the case of fluorescein, an aminohexanoyl spacer had to be inserted. Promastigotes of *L. infantum* were incubated with the compounds at a concentration of 60 μM for 1h and, after washings, observed by confocal microscopy. The fluorescein-labelled **63** analogue was found to not significantly penetrate into the parasites, while the two fluorescent versions of the longest peptide (i.e. **64** and **65** = doubling of the **63** sequence) were toxic, yielding rounded and immotile cells. However, all other fluorescent MPPs labelled cells in a more or less homogeneous fashion, indicating cytoplasmic as well as possible mitochondrial localization (see Figure S3). To get more insight into their localization, cell labelling by **67**, composed of

three units of the dipeptide Cha-arg, was compared to that obtained with mitotracker (Figure 3). Compound **67** was shown to enter the parasite and merged images indicate that it could at least partially localize to the mitochondrion.

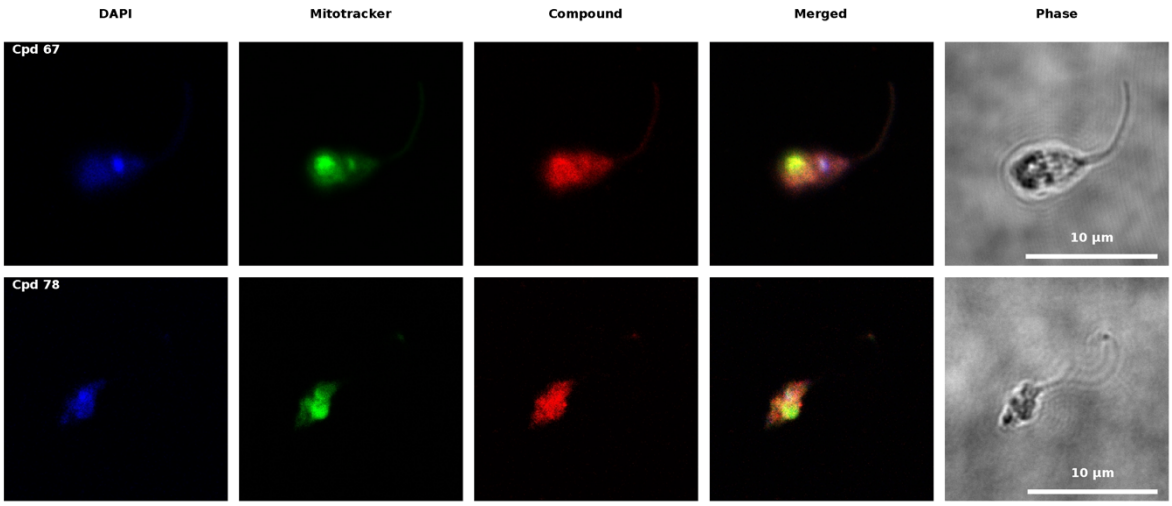

Figure 3. Penetration of **67** (top) and of the conjugate **78** (bottom) in promastigotes of *L. infantum*. Parasites were re-suspended in complete Schneider's medium and incubated with compounds (60 µM) at 26 °C for 3h in the dark. Cells were then washed, fixed, stained for DAPI and Mitotracker as described in Experimental Procedures and observed under confocal microscopy. Selected images are shown.

Having checked that MPPs could indeed penetrate the parasite, we prepared several conjugates containing the $(Cha\text{-}arg)_n$ MPP (n = 2, 3) (Table 5).

We first assessed their ability to activate isolated LmHslV (Table 5). The LmC6-U2 conjugates with a $(Cha\text{-}arg)_2$ (**69**) or a $(Cha\text{-}arg)_3$ (**72**) MPP were found to be about 67% and 48% as potent as **1** (LmC12-U2), and three and two-fold more potent than LmC6-U2 (**48**, Table 1), respectively. Thus, *N*-terminal lengthening increased potency despite the presence of several *D*-amino acid residues in the MPP sequence. However, **72** with the longest MPP was slightly less potent than **69**. As expected, the corresponding [Ala^{12}] analogues **70** and **73** were inactive. The [Chg^{11}]-LmC6-U2 conjugates behaved differently. Whereas **71** with a $(Cha\text{-}arg)_2$ MPP was only slightly less potent than the corresponding hexapeptide **50** (Table 3), adding a Cha-arg unit (**74**) led to a significant drop in activity with **74** being about 50% as active as [Chg^{11}]-LmC6-U2 (**50**), suggesting that the MPP segment significantly counteracted the favourable effect of Chg^{11}. In any case, **74** was found about 1.5-, 7- and 3-fold more potent than LmC12-U2 (**1**), LmC6-U2 (**48**), and **72** respectively. Finally, as already observed for **24** and **27** (Table 1), **75**, the [Ala^{12}] analogue of **74**, showed significant activating potency,

being 30% as active as **74**, and as active as **72**. Therefore, in contrast to **70** and **73**, **75** could not be used as a negative control in the following experiments.

Table 5. LmC6-U2 conjugates 69-78 with (Cha-arg)$_n$ MPP (n = 2, 3) and their LmHslV activation potency

Cpd	Structure	Relative potency (%)[a]
69	Ac-(*Cha-arg)$_2$*-Leu-Ala-Lys-Tyr-Leu-Leu-OH	67 ± 9
70	Ac-(*Cha-arg)$_2$*-Leu-Ala-Lys-Tyr-Leu-**Ala**-OH	NA[b]
71	Ac-(*Cha-arg)$_2$*-Leu-Ala-Lys-Tyr- **Chg**-Leu-OH	269 ± 26
72	Ac-(*Cha-arg)$_3$*-Leu-Ala-Lys-Tyr-Leu-Leu-OH	48 ± 6
73	Ac-(*Cha-arg)$_3$*-Leu-Ala-Lys-Tyr-Leu-**Ala**-OH	NA
74	Ac-(*Cha-arg)$_3$*-Leu-Ala-Lys-Tyr- **Chg**-Leu-OH	148 ± 20
75	Ac-(*Cha-arg)$_3$*-Leu-Ala-Lys-Tyr- **Chg-Ala**-OH	47 ± 5
76	Ac-*Cha-arg-Cha-arg*-NH_2	ND
77	Ac-*Cha-arg-Cha-arg-Cha-arg*-NH_2	ND
78	TO-(*Cha-arg)$_3$*- Leu-Ala-Lys-Tyr- **Chg**-Leu-OH	ND[c]

[a]Percentage of initial velocity relative to compound **1** (100%). LmHslV (2 µg, 75.2 nM) was incubated at 37 °C with 100 µM JMV4482 (Z-EVNL-AMC) in the presence of 500 µM peptides. The fluorescence of the free AMC group, proportional to the activity of the sample, was measured at 2 min. intervals. [b]NA = No activity (≤5%). [c]ND = Not determined.

Next, the toxicity toward the human monocytic cell line THP-1 of all conjugates (excepted **75**), the MPP's alone **76** and **77**, and the peptides LmC12-U2 (**1**), LmC6-U2 (**48**) and [Chg^{11}]-LmC12-U2 (**24**), was assessed after 48h incubation. As presented in Figure 4A (not shown for **1**, **24**, **48** and **70**), no compound showed toxicity at 60 µM concentration.

Finally, the same compounds were tested in cultures of the promastigote form of *L. infantum* (Figure 4B). As expected, no non-conjugated peptides (i.e. **1**, **24**, **48**, not shown in Figure 4B for the sake of clarity) and no vector alone (i.e. **76**, **77**) were found toxic for the parasite after 48h incubation at a 60 µM concentration. The LmC6-U2 conjugate with two Cha-arg units (**69**) was also inactive, as of course its [Ala^{12}] analogue **70** (not shown in Figure 4B). The more potent [Chg^{11}] analogue **71** showed some activity with about 35% growth inhibition at 60 µM. More significant effects were found for conjugates containing three Cha-arg units. The corresponding LmC6-U2 conjugate **72** inhibited parasite growth by 65% at 30 µM and maximally (about 80% inhibition) at 60 µM. As expected, its [Ala^{12}] analogue **73** showed no

significant toxicity. Finally, the more potent [Chg[11]] analogue **74** showed higher activity with 65% inhibition at 15 µM and maximally at 30 µM.

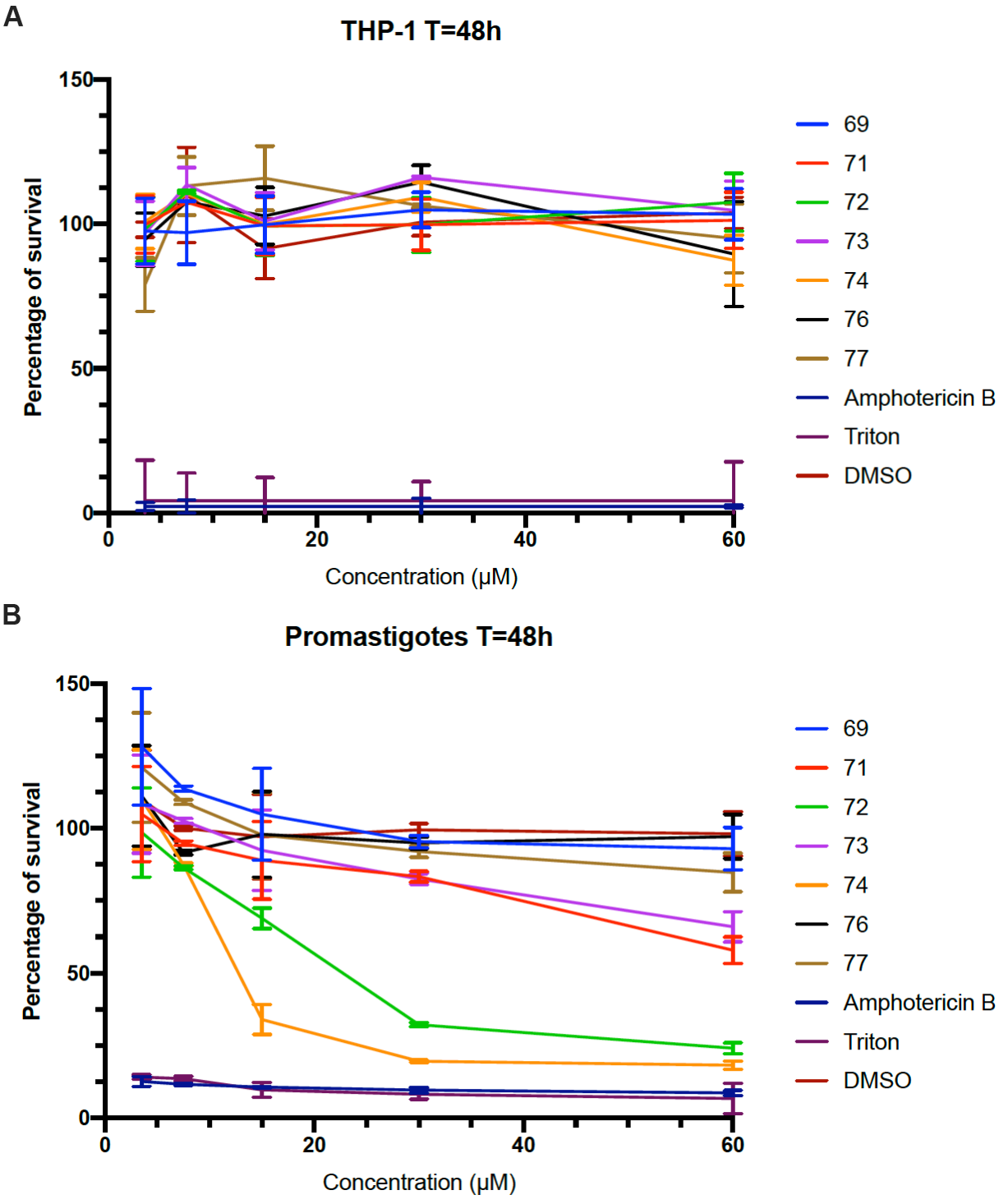

Figure 4. A) Toxicity of compounds toward human THP-1 cells after 48h and at concentrations up to 60 µM. B) Toxicity of compounds toward the promastigote form of *L. infantum* after 48h and at concentrations up to 60 µM.

Overall, these results suggested that a C-terminal HslU peptide conjugated to an MPP may indeed inhibit parasite growth, and that a minimum of three Cha-arg units is necessary for efficient vectorization. A fluorescently labelled analogue of **74**, **78**, was shown to penetrate into *L. infantum* promastigotes with similar localization as the fluorescent vector **67** (Figure 3). Compared to **67**, the parasite appeared damaged after 3h incubation with **78**, suggesting that some toxicity occurred in agreement with the observed toxicity of the non-fluorescent analogue **74** (Figure 4B).

3. Conclusion

We performed the first steps toward the development of peptidomimetics potentially able to inhibit the interaction between the LmHslU and LmHslV complexes. By substituting essential residues of the reference peptide LmC12-U2 **1** (i.e. 5 out of the 6 C-terminal residues) with structurally close amino acids, we identified up to three-fold more potent analogues. In particular, substitution at positions 10 and 11 afforded the largest improvements. More particularly, a Chg at position 11 (Cpd **24**) resulted in the most dramatic effect. This particular behaviour was also observed in the LmC6-U2 and cyclic LmC9-U2 series. Indeed the [Chg^{11}]-LmC6-U2 analogue **50** was found only slightly less potent than the corresponding dodecapeptide **24**, in strong contrast with LmC6-U2 **48** whose activity was about six times lower than that of LmC12-U2 **1**. The reason why the Chg residue is so favourable is not clear but its higher rigidity could lead to more favourable binding kinetics. Finally, we found that the conjugate **74**, derived from compound **50** and incorporating a known mitochondrial penetrating peptide (i.e. $(Cha\text{-}arg)_3$) inhibited the growth of the parasite promastigote form with a maximal effect at 30 μM, while it did not show any toxicity toward human THP-1 cells at the same concentration. **78**, a fluorescent analogue of **74**, confirmed the ability of the conjugate to penetrate the parasite. Future efforts will focus on the design of C-ter HslU peptidomimetics with enhanced metabolic stability.

4. Experimental

Reagents and resins for peptide synthesis (Fmoc-protected amino acids, HATU, DIEA, TFA, piperidine, 2-chlorotrityl chloride (1.6 mmol/g) and Fmoc-Rink amide (0.56 mmol/g) polystyrene resins, solvents and other reagents) were purchased from Iris-Biotech, Merck/Novabiochem, Bachem, Riedel-de Haën, Carlo-Erba, Merck/Sigma-Aldrich or Alfa-Aesar, and used without further purification. Solvents used for RP-HPLC and LC-MS were of HPLC grade.

4.1. Synthesis.

All peptides were assembled either on a 2-chloro-trityl resin (Tables 1-3, 5, S1, S3) or on a Rink amide resin (compounds **59-68**, Tables 4, S2), following either manual or microwave-assisted solid phase synthetic protocols with Fmoc as the *N*α-protecting group and HBTU or HATU/DIEA as coupling agents. Their synthesis as well that of the substrate JMV4482 (Z-EVNL-AMC) used for activity tests are described in [27].

4.2. Enzymatic assays.

LmHslV was expressed in *E. coli*, and purified as previously described [27]. The peptidase activity of recombinant LmHslV was assessed by measuring the fluorescence of AMC released after hydrolysis of the fluorogenic substrate JMV4482 (Z-EVNL-AMC), 100 µM. LmHslV activation was obtained by addition of activating peptides (see type and concentration in the figure legends). Activity buffer: 25 mM Tris-HCl pH 8.0, 1mM DTT, 0.5mM EDTA and 5mM $MgCl_2$. Most of the experiments were performed in a final volume of 50 µl in black 96-well microplates (Fisher Scientific Bioblock, City, Country). Fluorescence was measured using a spectrofluorimeter (BIO-TEK Instrument, Inc., City, Country): filters 360/340 for excitation and 460/440 for emission.

4.3. Cell assays.

4.3.1. Cultures of L. infantum (promastigote form).

L. infantum MON-1 (MHOM/FR/94/LPN101) was isolated from a patient with Mediterranean visceral leishmaniasis contracted in the Nice area (South of France). *L. infantum* promastigotes were routinely grown at 26°C in Parasite medium based on Schneider's Insect Medium (Sigma®) supplemented with $NaHCO_3$ 0.4g/L (Janssen chimica®), $CaCl_2$ 0.6g/L (Fluka Chemika®), fetal bovine serum 10% (Gibco®), 10 mL urine pool for 500 mL of medium, Phenol Red 0.1%, Hepes 1M pH 7.3, penicillin/streptomycin 1% (Gibco®), and L-Glutamine 1% (Gibco®). Adequate metacyclogenesis was obtained after 5-day-old late-log-phase and metacyclic promastigotes were used for microscopy experiment.

4.3.2. Cultures of THP-1 cells.

The THP-1 cell line (ATCC TIB-202) was routinely grown in RPMI 1640 medium containing 10% fetal calf serum, penicillin/streptomycin 1% (Gibco®), and L-Glutamine 1% (Gibco®). at 37°C, 5% CO_2 (THP-1 medium).

4.3.3. Confocal microscopy.

After parasite counting by nephelometry, an adequate volume of parasite culture (10^7 parasites per mL for one condition) was placed in a sterile 50 mL tube. After centrifugation (3 min at 3600 rpm), the supernatant was gently removed and re-suspended in complete Schneider's medium. One mL suspension per condition was introduced in an Eppendorf tube and peptide solution in DMSO was added to a 60 μM final concentration. After homogenisation, the tubes were incubated at 26 °C and in the dark for 1h. The tubes were then centrifuged (3 min at 3600 rpm) and the supernatant gently removed. For washing, 1 mL of 1X PBS was added and the resulting suspension again centrifuged (3 min at 3600 rpm) and the supernatant removed. For cell fixation, 1 mL of 1X PBS containing 4% paraformaldehyde was added and the tubes were incubated at 26 °C for 1h30. After centrifugation (3 min at 3600 rpm) and gentle removal of the supernatant, 1 mL of 1X PBS was added (washing) and a portion of the suspension was placed on a microscope slide, which was examined with a Zeiss LSM 510-META confocal laser scanning microscope. To observe the fluorescence of thiazole orange- and fluorescein-labelled peptides, $\lambda_{exc/em}$ were 512/533 nm and 488/525 nm, respectively. To observe DAPI and Mitotracker, $\lambda_{exc/em}$ were 405/460 nm and 488/525, respectively.

4.3.4. Toxicity assays toward THP-1 cells.

After cell counting by nephelometry, a defined volume of cell suspension was centrifugated (5 min at 10,000 rpm), the supernatant removed and the pellet was diluted to a concentration of 5.10^5 cells/mL with THP-1 medium containing 20 ng/mL of PMA (phorbol 12-myristate-13-acetate) to activate THP-1. After homogenization, the suspension was distributed in a 96-wells plate (100 μL per well) and the cultures incubated at 37 °C under 5% CO_2 atmosphere for 24h. A serial dilution (3.75, 7.50, 15, 30 and 60 μM) of compounds was applied on the cultures, which were then incubated for 48h in an incubator at 37 °C in a humidified atmosphere containing 5% CO_2. Cell viability was finally assessed by Alamar Blue assay. 10 μL of Alamar Blue solution was added to each well and reading was performed using a plate reader after 3h ($\lambda_{exc/em}$ = 530/590 nm). Each experiment was repeated three times.

4.3.5. Toxicity assays toward L. infantum (promastigote form).

After cell counting by nephelometry, a defined volume of cell suspension to have 2.10^5 parasites per well was centrifugated (5 min at 10,000 rpm), the supernatant removed, and the pellet was diluted to a concentration of 2.10^6 cells/mL with parasite medium. After homogenization, the suspension was distributed in a 96-wells plate (100 μL per well). A serial

dilution (3.75, 7.50, 15, 30 and 60 μM) of compounds was applied on the cultures, and plates were sealed with parafilm and incubated for 48h at 26 °C. Cell viability was finally assessed by a bioluminescence assay. 20 μL of a 30 mg/mL solution of luciferin was added to each well and the bioluminescence was rapidly measured using a plate reader Synergy 2 (Bio Tek). Each experiment was repeated three times.

Acknowledgments.

We thank the Infectiopole Sud Foundation (IHU Méditerranée Infection, Marseille, France) for allocating post-doctoral fellowships to P.S. and K.S. N.M.K was supported by a doctoral contract from Montpellier University, a stipend from the CRBM and a fellowship from the FRM (Fondation pour la Recherche Médicale). We also thank Pierre Sanchez for mass spectrometry analyses.

Appendix A. Supplementary material

Synthesis, Analysis and purification, characteristics of synthetic compounds (Tables S1-S3), CD experiments (Fig. S1, Table S4), molecular modelling (protocol, model of [Chg^{11}]-C8-U2 binding to HslV (Fig. S2)), confocal microscopy study of labelled MPPs in *L. infantum* (Fig. S3),

References.

[1] L. Maxfield, J. S. Crane, Leishmaniasis. In: *StatPearls*, Treasure Island (FL), (2020). Can be fund under https://www.ncbi.nlm.nih.gov/books/NBK531456/

[2] J. A. L. Lindoso, C. H. V. Moreira, M. A. Cunha, I. T. Queiroz, Visceral leishmaniasis and HIV coinfection: current perspectives, HIV AIDS 10 (2018) 193-201. DOI: 10.2147/HIV.S143929

[3] P. P. Simarro, G. Cecchi, J. R. Franco, M. Paone, A. Diarra, J. A. Ruiz-Postigo, E. M. Fèvre, R. C. Mattioli, J. G. Jannin, Estimating and mapping the population at risk of sleeping sickness, PLoS Negl. Trop. Dis. 6 (2012) e1859. DOI: 10.1371/journal.pntd.0001859

[4] B. Zingales, Trypanosoma cruzi genetic diversity: Something new for something known about Chagas disease manifestations, serodiagnosis and drug sensitivity, Acta Trop. 184 (2018), 38-52. DOI: 10.1016/j.actatropica.2017.09.017

[5] M. P. Barrett, R. J. Burchmore, A. Stich, J. O. Lazzari, A. C. Frasch, J. J. Cazzulo, S. Krishna, The trypanosomiases, Lancet 362 (2003) 1469-1480. DOI: 10.1016/S0140-

6736(03)14694-6

[6] R. Brun, J. Blum, F. Chappuis, C. Burri, Human African trypanosomiasis, Lancet 375 (2010) 148-159. DOI : 10.1016/S0140-6736(09)60829-1

[7] K. Seifert, Structures, targets and recent approaches in anti-leishmanial drug discovery and development, Open Med. Chem. J. 5 (2011) 31-39. DOI: 10.2174/1874104501105010031

[8] M. Berriman, E. Ghedin, C. Hertz-Fowler, G. Blandin, H. Renauld, D. C. Bartholomeu, N. J. Lennard et al., The genome of the African trypanosome *Trypanosoma brucei*, Science 309 (2005) 416-422. DOI: 10.1126/science.1112642

[9] N. M. El-Sayed, P. J. Myler, D. C. Bartholomeu, D. Nilsson, G. Aggarwal, A.-N. Tran et al., The genome sequence of *Trypanosoma cruzi*, etiologic agent of Chagas disease, Science 309 (2005) 409-415. DOI: 10.1126/science.1112631

[10] A. C. Ivens, C. S. Peacock, E. A. Worthey, L. Murphy, G. Aggarwal, M. Berriman, et al., The genome of the kinetoplastid parasite, *Leishmania major*, Science 309 (2005) 436-442. DOI: 10.1126/science.1112680

[11] E. Castillo, M. A. Dea-Ayuela, F. Bolas-Fernandez, M. Rangel, M. E. Gonzalez-Rosende, The kinetoplastid chemotherapy revisited: current drugs, recent advances and future perspectives, Curr. Med. Chem. 17 (2010) 4027-4051. DOI: 10.2174/092986710793205345

[12] M. Rohrwild, O. Coux, H. C. Huang, R. P. Moerschell, S. J. Yoo, J. H. Seol, C. H. Chung, A. L. Goldberg, HslV-HslU: A novel ATP-dependent protease complex in *Escherichia coli* related to the eukaryotic proteasome, Proc. Natl. Acad. Sci. USA 93 (1996) 5808-5813. DOI: 10.1073/pnas.93.12.5808

[13] D. Missiakas, F. Schwager, J. M. Betton, C. Georgopoulos, S. Raina, Identification and characterization of HsIV HsIU (ClpQ ClpY) proteins involved in overall proteolysis of misfolded proteins in *Escherichia coli*, EMBO J. 15 (1996) 6899–6909. PMCID: PMC452516

[14] S. J. Yoo, J. H. Seol, D. H. Shin, M. Rohrwild, M. S. Kang, K. Tanaka, A. L. Goldberg, C. H. Chung, Purification and characterization of the heat shock proteins HslV and HslU that form a new ATP-dependent protease in *Escherichia coli*, J. Biol. Chem. 271 (1996) 14035–14040. DOI: 10.1074/jbc.271.24.14035

[15] B. Mordmüller, R. Fendel, A. Kreidenweiss, C. Gille, G. C. Hurwitz, W. G. Metzger, J. F. Kun, T. Lamkemeyer, A. Nordheim, P. G. Kremsner, Plasmodia express two threonine-peptidase complexes during asexual development, Mol. Biochem. Parasitol. 148 (2006) 79-85. DOI: 10.1016/j.molbiopara.2006.03.001

[16] S. Jain, S. Rathore, M. Asad, M. E. Hossain, D. Sinha, G. Datta, A. Mohmmed, The

prokaryotic ClpQ protease plays a key role in growth and development of mitochondria in *Plasmodium falciparum*, Cell. Microbiol. 15 (2013) 1660-1673. DOI: 10.1111/cmi.12142

[17] B. Couvreur, R. Wattiez, A. Bollen, P. Falmagne, D. Le Ray, J. C. Dujardin, Eubacterial HslV and HslU subunits homologs in primordial eukaryotes, Mol. Biol. Evol. 19 (2002) 2110-2117. DOI: 10.1093/oxfordjournals.molbev.a004036

[18] Z. Li, M. E. Lindsay, S. A. Motyka, P. T. Englund, C. C. Wang, Identification of a bacterial-like HslVU protease in the mitochondria of *Trypanosoma brucei* and its role in mitochondrial DNA replication, PLoS Pathogens 4 (2008) e1000048. DOI: 10.1371/journal.ppat.1000048

[19] S. Tschan, A. Kreidenweiss, Y. D. Stierhof, N. Sessler, R. Fendel, B. Mordmüller, Mitochondrial localization of the threonine peptidase PfHslV, a ClpQ ortholog in *Plasmodium falciparum*, Int. J. Parasitol. 40 (2010) 1517-1523. DOI : 10.1016/j.ijpara.2010.05.006

[20] D.-E. Mbang, Y. Sterkers, C. Morelle, N.-M. Kebe, L. Crobu, P. Portalès, O. Coux, J.-F. Hernandez, S. Meghamla, M. Pagès, P. Bastien, The bacterial-like HslVU protease complex subunits are involved in the control of different cell cycle events in trypanosomatids, Acta Trop. 131 (2014) 22-31. DOI: 10.1016/j.actatropica.2013.11.017

[21] M. C. Sousa, C. B. Trame, H. Tsuruta, S. M. Wilbanks, V. S. Reddy, D. B. McKay, Crystal and solution structures of an HslUV protease-chaperone complex, Cell 103 (2000) 633-643. DOI: 10.1016/s0092-8674(00)00166-5

[22] J. Wang, J. J. Song, M. C. Franklin, S. Kamtekar, Y. J. Im, S. H. Rho, I. S. Seong, C. S. Lee, C. H. Chung, S. H. Eom, Crystal structures of the HslVU peptidase-ATPase complex reveal an ATP-dependent proteolysis mechanism, Structure 9 (2001) 177-184. DOI: 10.1016/s0969-2126(01)00570-6

[23] R. Ramachandran, C. Hartmann, H. K. Song, R. Huber, M. Bochtler, Functional interactions of HslV (ClpQ) with the ATPase HslU (ClpY), Proc. Natl. Acad. Sci. USA 99 (2002) 7396-7401. DOI: 10.1073/pnas.102188799

[24] I. S. Seong, M. S. Kang, M. K. Choi, J. W. Lee, O. J. Koh, J. Wang, S. H. Eom, C. H. Chung, The C-terminal tails of HslU ATPase act as a molecular switch for activation of HslV peptidase, J. Biol. Chem. 277 (2002) 25976-25982. DOI: 10.1074/jbc.M202793200

[25] M. C. Sousa, B. M. Kessler, H. S. Overkleeft, D. B. McKay, Crystal structure of HslUV complexed with a vinyl sulfone inhibitor: corroboration of a proposed mechanism of allosteric activation of HslV by HslU, J. Mol. Biol. 318 (2002) 779-785. 10.1016/S0022-2836(02)00145-6

[26] L. Shi, L. E. Kay, Tracing an allosteric pathway regulating the activity of the HslV

protease, Proc. Natl. Acad. Sci. USA 111 (2014) 2140-2145. DOI: 10.1073/pnas.1318476111

[27] N. M. Kebe, K. Samanta, P. Singh, J. Lai-Kee-Him, V. Apicella, N. Payrot, N. Lauraire, B. Legrand, V. Lisowski, D.-E. Mbang-Benet, M. Pages, P. Bastien, A. V. Kajava, P. Bron, J.-F. Hernandez, O. Coux, The HslV Protease from *Leishmania major* and Its Activation by C-terminal HslU Peptides, Int. J. Mol. Sci. 20 (2019) 1021. DOI: 10.3390/ijms20051021

[28] M. K. Azim, W. Goehring, H. K. Song, R. Ramachandran, M. Bochtler, P. Goettig, Characterization of the HslU chaperone affinity for HslV protease, Protein Sci. 14 (2005) 1357-1362. DOI: 10.1110/ps.04970405

[29] M. Bochtler, C. Hartmann, H. K. Song, G. P. Bourenkov, H. D. Bartunik, R. Hubert, The structures of HsIU and the ATP-dependent protease HsIU-HsIV, Nature 403 (2000) 800-805. DOI: 10.1038/35001629

[30] S. Rathore, S. Jain, D. Sinha, M. Gupta, M. Asad, A. Srivastava, M. S. Narayanan, G. Ramasamy, V. S. Chauhan, D. Gupta, A. Mohmmed, Disruption of a mitochondrial protease machinery in Plasmodium falciparum is an intrinsic signal for parasite cell death, Cell Death Dis. 2 (2011) e231. DOI: 10.1038/cddis.2011.118

[31] K. H. Sung, S. Y. Lee, H. K. Song, Structural and biochemical analyses of the eukaryotic heat shock locus V (HslV) from *Trypanosoma brucei*, J. Biol. Chem. 288 (2013) 23234-23243. DOI: 10.1074/jbc.M113.484832

[32] G. R. Marshal, H. E. Bosshard, Angiotensin II. Studies on the biologically active conformation, Circ. Res. Suppl. II 30/31 (1972) 143-150. PMID: 4341473.

[33] A. W. Burgess, S. W. Leach, An obligatory alpha-helical amino acid residue, Biopolymers 12 (1973) 2599-2605. DOI: 10.1002/bip.1973.360121112

[34] T. S. Sudha, P. Balaram, Stabilization of beta-turn conformations in enkephalins. alpha-Aminoisobutyric acid analogs, Int. J. Pept. Protein Res. 21 (1983) 381-38. DOI : 10.1111/j.1399-3011.1983.tb03119.x

[35] E. Benedetti, B. Di Blasio, V. Pavone, C. Pedone, A. Santini, M. Crisma, G. Valle, C. Toniolo, Structural versatility of peptides from $C^{\alpha,\alpha}$dialkylated glycines: Linear Ac_3c homo-oligopeptides, Biopolymers 28 (1989) 175-184. https://doi.org/10.1002/bip.360280119

[36] J. W. Payne, R. Jakes, B. S. Hartley, The primary structure of alamethicin, Biochem. J. 117 (1970) 757-766. DOI: 10.1042/bj1170757

[37] L. E. LeDuc, G. R. Marshall, P. Needleman, Differentiation of bradykinin receptors and of kininases with conformational analogues of bradykinin, Mol. Pharmacol. 14 (1978) 413-421. PMID: 207969.

[38] J. W. Taylor, The synthesis and study of side-chain lactam-bridged peptides,

Biopolymers Pept. Sci. 66 (2002) 49-75. DOI: 10.1002/bip.10203

[39] M. E. Houston, C. L. Gannon, C. M. Kay, R. S. Hodges, Lactam bridge stabilization of alpha-helical peptides: ring size, orientation and positional effects, J. Pept. Sci. 1 (1995) 274-282. DOI: 10.1002/psc.310010408

[40] H. E. Dayringer, A. Tramontano, S. R. Sprang, R. J. Fletterick, Interactive program for visualization and modelling of proteins, nucleic acids and small molecules, J. Mol. Graph. 4 (1986) 82–87. DOI: https://doi.org/10.1016/0263-7855(86)80002-9

[41] K. Zhao, G. M. Zhao, D. Wu, Y. Soong, A. V. Birk, P. W. Schiller, H. H. Szeto, Cell-permeable peptide antioxidants targeted to inner mitochondrial membrane inhibit mitochondrial swelling, oxidative cell death, and reperfusion injury, J. Biol. Chem. 279 (2004) 34682-34690. DOI: 10.1074/jbc.M402999200

[42] K. L. Horton, K. M. Stewart, S. B. Fonseca, Q. Guo, S. O. Kelley, Mitochondira-penetrating peptides, Chem. Biol. 15 (2008) 375-382. DOI: 10.1016/j.chembiol.2008.03.015

[43] L. F. Yousif, K. M. Stewart, K. L. Horton, S.O. Kelley, Mitochondria-penetrating peptides: sequence effects and model cargo transport, ChemBioChem 10 (2009) 2081-2088. DOI: 10.1002/cbic.200900017

[44] S. O. Kelley, K. M. Stewart, R. Mourtada, Development of novel peptides for mitochondrial drug delivery: amino acids featuring delocalized lipophilic cations, Pharm. Res. 28 (2011) 2808-2819. DOI: 10.1007/s11095-011-0530-6

[45] J. R. Carreon, K. M. Stewart, K. P. Mahon Jr., S. Shin, S. O. Kelley, Cyanine dye conjugates as probes for live cell imaging, Bioorg. Med. Chem. Lett. 17 (2007) 5182-5185. DOI: 10.1016/j.bmcl.2007.06.097

[46] K. L. Horton, M. P. Pereira, K. M. Stewart, S. B. Fonseca, S. O. Kelley, Tuning the activity of mitochondria-penetrating peptides for delivery or disruption, ChemBioChem 13 (2012) 476-485. DOI: 10.1002/cbic.201100415

Table of Contents graphical abstract.

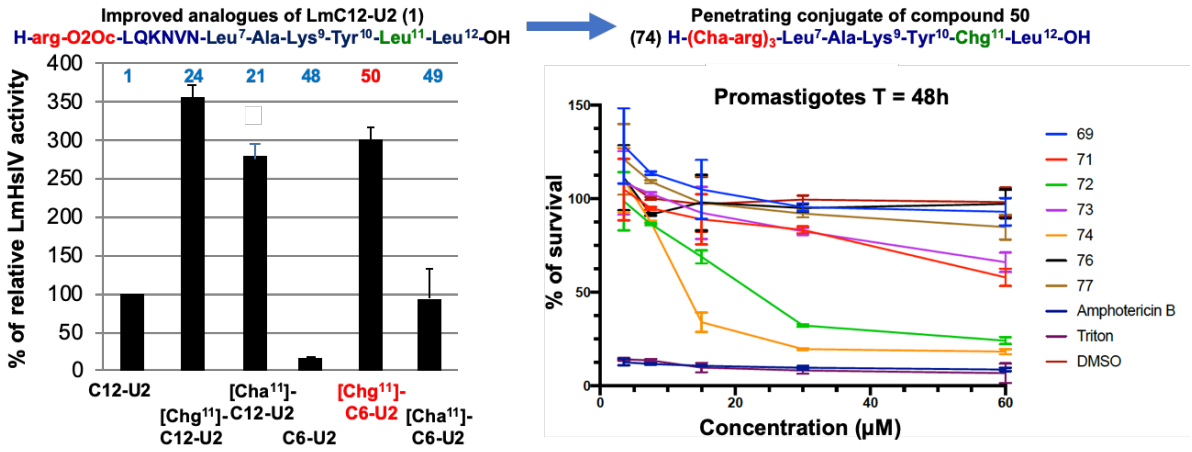

Highlights

- The HslVU protease of Trypanosomatids is a potential drug target.
- We developed LmHslU C-terminal-derived peptides binding to LmHslV and potentially inhibiting HslVU assembly.
- A SAR study of the C-terminal LmHslU dodecapeptide identified a potent hexapeptide.
- Conjugated to a penetrating peptide, it was found to be toxic to parasites in culture.
- The fluorescently-labelled conjugate entered the promastigote form of *L. infantum*.